Journal of Power Sources 185 (2008) 1267–1271

Contents lists available at ScienceDirect

Journal of Power Sources

journal homepage: www.elsevier.com/locate/jpowsour

Short communication

Measurement of the water transport rate in a proton exchange membrane fuel cell and the influence of the gas diffusion layer

Wei Dai [a,b], Haijiang Wang [a,*], Xiao Zi Yuan [a], Jonathan J. Martin [a], Zhiping Luo [b], Mu Pan [b]

[a] Institute for Fuel Cell Innovation, National Research Council Canada, 4250 Wesbrook Mall, Vancouver, BC, Canada V6T 1W5
[b] State Key Laboratory of Advanced Technology for Materials Synthesis and Processing, Wuhan University of Technology, 122 Luoshi Road, Wuhan 430070, PR China

ARTICLE INFO

Article history:
Received 5 June 2008
Received in revised form 11 July 2008
Accepted 15 July 2008
Available online 25 July 2008

Keywords:
PEM fuel cell
Water transport
Gas diffusion layer (GDL)
Flooding

ABSTRACT

Water management in a PEM fuel cell significantly affects the fuel cell performance and durability. The gas diffusion layer (GDL) of a PEM fuel cell plays a critical role in the water management process. In this short communication, we report a simple method to measure the water transport rate across the GDL. Water rejection rates across a GDL at different cathode air-flow rates were measured. Based on the measurement results, the fuel cell operating conditions, such as current density, temperature, air stoichiometry and relative humidity, corresponding to membrane drying and flooding conditions were identified for the particular GDL used. This method can help researchers develop GDLs for a particular fuel cell design with specific operating conditions and optimize the operation conditions for the given PEM fuel cell components.

1. Introduction

Water management in a PEM fuel cell significantly affects the fuel cell performance and durability. In a PEM fuel cell, water is generated by the oxygen reduction reaction (ORR) at the cathode and excessive water is removed by the reactant flow. For the current PEM fuel cell technology, the proton conductivity of the membrane, which impacts the efficiency of the fuel cell's electrochemical reaction, highly depends on the water content of the membrane. If the membrane is dry, it leads to a performance drop or, under extreme conditions, even physical damage to the membrane. If the excessive water cannot be removed efficiently, liquid water floods the electrodes and the flow channels, interfering with the reactant mass transfer. Optimizing water balance in a PEM fuel cell, so as to avoid drying or flooding is critical for maintaining the performance and durability of the cell.

Many efforts have been made to investigate water transport and balance in PEM fuel cells. Researches have focused on water transport in the membrane [1–11], gas diffusion layer (GDL) [12–17], flow field channels [18–22] and their effects on fuel cell performance. Experiments [15–17,23–25] and model simulations [26–31] have proven that, besides the membrane, the GDL is an important component for water management, especially for water removal. The GDL is a conductive porous layer, between the flow channel and the catalyst layer, providing gas and water transport channels, current collection, as well as a membrane protection. The main research areas on water transport in GDLs include study of GDL properties, such as polytetrafluoroethylene (PTFE) content [14,32], GDL porosity [24,25] and permeability [23], PTFE content and carbon loading of the micro-porous layer (MPL) [13,14,17,28,30,32–42], and the use of transparent cells and neutron imaging to monitor liquid water formation and movement [43–48].

Although GDLs play a critical role on water management in PEM fuel cells, there is a lack of experimental data focusing on and investigating the effects of the GDL on water transport. To optimize the PEM fuel cell design, water transport data in the GDL, as well as in the membrane and flow channels, is necessary. In this paper, the effects of the GDL on water transport in PEM fuel cells were investigated. Measurements of water transport properties with and without GDLs and under different conditions were carried out.

2. Experimental

2.1. Cell components and assembly

The water transport properties of GDLs were measured using a real PEM fuel cell setup. All of the cell components and assembling processes were the same as those of an operating PEM fuel cell except that the regular MEA was replaced with a piece of membrane with/without GDL. The cell hardware was a Tandem® TP50 50 cm^2 single cell with a single serpentine channel for the anode flow field, dual parallel serpentine channels for the cathode flow field. The

* Corresponding author. Fax: +1 604 221 3001.
E-mail address: haijiang.wang@nrc-cnrc.gc.ca (H. Wang).

0378-7753/$ – see front matter.
doi:10.1016/j.jpowsour.2008.07.033

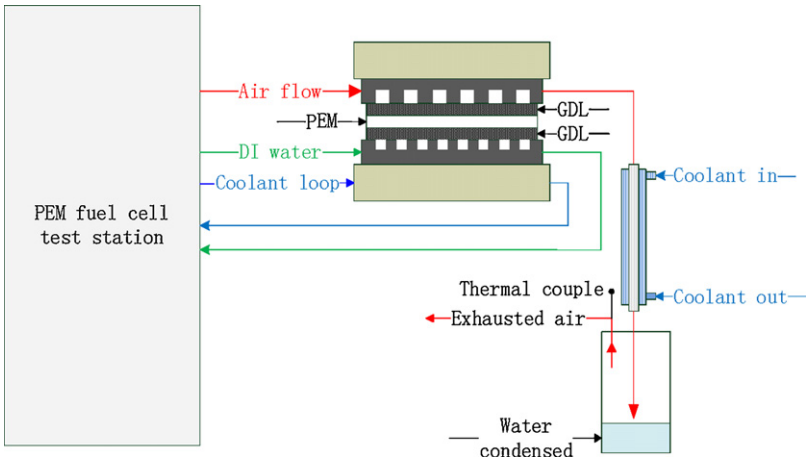

Fig. 1. The schematic of the experimental setup for the water transport measurement (The air at "cathode", the deionized water in "anode" and coolant temperatures were kept in the same temperature.).

cathode channels were 0.889 mm deep, 1.499 mm wide at the top of the channel (closest to the GDL) and 1.016 mm wide at the bottom, while the land was 1.041 mm wide on the plate surface.

The membrane used was Nafion® 211CS from DuPont® (DuPont, USA) with a thickness of 25 μm. Polyimide film with silicon adhesive on one side was used as the sub-gasket to protect the edges of the Nafion® membrane. TORAY® TGPH-060 carbon fiber paper (190 μm thick) was used for the GDL. The GDLs were treated with 40-wt% PTFE and were provided by E-TEK® (E-TEK, USA). A homemade die cutter was used to cut the GDLs, membranes and sub-gaskets. The polyimide sub-gaskets were bonded to both sides of Nafion® membrane, leaving an "active" area of 7 cm × 7 cm. The 40-wt% PTFE-treated GDLs were used on the "cathode" side. To balance the membrane stress from each side, the plain GDLs (without wet proofing) were put on the "anode" side. The cell assembly was compressed using N_2 gas at 100 psi and leak testing was performed after each assembly and before the measurements.

2.2. Water transport measurement

The cell was operated on a FuelCon® test station (FuelCon, Germany) allowing for control of air-flow rate, air temperature, and coolant temperature. At the "cathode", air was fed with a controlled humidity provided by the test station's bubbler humidifier. Deionized water was fed to the "anode" using a peristaltic pump. Since the deionized water at the "anode" side could easily transport through the plain GDLs, the membrane remained fully hydrated during the test. The air, coolant and anode-side deionized water were kept at the same temperature.

Water transported through the membrane and GDL and then subsequently removed by the air-flow was condensed in a high-efficiency, water-cooled condenser and collected using a reservoir bottle. The temperature of the exhausted air was measured after it exited the reservoir bottle. The schematic of the whole measurement setup is depicted in Fig. 1.

The quantity of water transported through the membrane and 40 wt% PTFE-treated GDL was measured at different air-flow rates (1.5, 2.0, 2.5. 3.0 and 3.5 SLPM (standard liter per minute)), under different air humidities (dry gas and dew point = 40, 50, 60, 70, and 80 °C) and at different temperatures (60, 70, and 80 °C). The water transport without GDL was also measured as a basis for comparison to explore the effect of GDL in water transport. Table 1 lists the relative humidity of the feed air at different operating temperatures.

Table 1
Relative humidities of the feed air

Air temperature (°C)	Air dew point temperature (°C)			
60	Dry (0% RH)	40 (37% RH)	50 (62% RH)	60 (100% RH)
70	Dry (0% RH)	50 (40% RH)	60 (64% RH)	70 (100% RH)
80	Dry (0% RH)	60 (42% RH)	70 (66% RH)	80 (100% RH)

2.3. Calculation of the actual water flux

Water collected (W_c) during measurement is related to the water flux (W_{flux}, defined as the rate of water transported through the membrane and GDL and then removed by the air-flow), the water in the humidified air (W_{in}), and the water in the exhausted air (W_{vap}). Then, the W_{flux} (g min^{-1}) can be calculated with Eq. (1). In Eq. (1), W_{in} was calculated by using the water saturation pressure at the humidified dew point temperature and W_{vap} was calculated by using the saturation pressure at the temperature of the exhausted air.

$$W_{flux} = W_c - W_{in} + W_{vap} \quad (1)$$

The theoretical water content (W_{satu}, g min^{-1}) in the saturated air at different temperatures (T, K) can be calculated by the saturated water vapor partial pressure (P_{satu}, Pa) as a function of air-flow (F_{air}, l min^{-1}). Based on the ideal gas equation:

$$W_{satu} = \frac{M_{water}}{t} = \frac{18 \times 10^{-3} F_{air} P_{satu}}{RT} \quad (2)$$

where R is the gas constant (8.314 J K^{-1} mol^{-1}); t is time (min); and M_{water} is the mass of water (g).

Water vapor from the air supply is neglectable in this experiment since the air supply from the lab facility has been filtered to remove contaminants and water vapor.

3. Results and discussion

3.1. Effects of hydrophobic GDLs on water transport

Fig. 2 compares the water flux with and without a GDL with 40-wt% PTFE under the condition of dry feed air at 70 °C. In Fig. 2, the dashed line is the theoretically calculated water content (W_{satu}) in saturated air at 70 °C as a function of flow rate. It is clearly seen that the measured water flux without GDL is higher than the water content in theoretically saturated air, which indicates that water vapor absorbed by the feed air exceeds the saturated level. Therefore, the excessive water will be condensed as liquid and then removed by

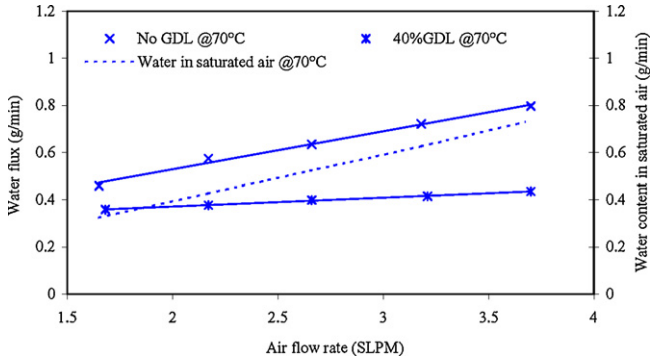

Fig. 2. Water flux using GDL treated by 40 wt% PTFE and without GDL under the condition of 70 °C dry feed air; PEM: Nafion® 211CS, 7 cm × 7 cm; GDL: TORAY® TGPH-060, 40 wt% PTFE-treated GDL on the cathode and plain GDL on anode; anode: deionized water, cathode: dry air.

the air-flow. Liquid water can clog the flow channel and lead to a flooding problem, which is a situation that needs to be avoided in a real PEM fuel cell. When the GDL with 40% PTFE is used, the water fluxes are lower than the water content in theoretically saturated air, which means the water transported across the GDL in the air-flow might be mostly in the form of vapor. The water fluxes with the given GDL are much lower than without the GDL at all testing flow rates, confirming that the GDL is the main water rejection barrier from the membrane. This can be attributed to the high hydrophobicity, resulting from the PTFE content in the GDL, leading to a higher capillary pressure across the interface of between the GDL and membrane, which restricts the water transport from the membrane surface through GDL to the flow channels. Similar results were observed at different temperatures, as shown in Fig. 3. At 60 °C, water fluxes using hydrophobic GDLs decrease around 30 ± 5% at different flow rates compared with those without the GDL. At 70 and 80 °C, the water fluxes decrease around 35 ± 10%.

Another interesting phenomenon in Fig. 3 is that with 40-wt% PTFE-treated GDL, the water fluxes as a function of flow rate are nearly linear, as listed in Eqs. (3)–(5) for different temperatures:

$$\text{At } 60\,^{\circ}\text{C}: W_{\text{flux}} = 0.0352F_{\text{air}} + 0.1671 \quad (3)$$

$$\text{At } 70\,^{\circ}\text{C}: W_{\text{flux}} = 0.0376F_{\text{air}} + 0.2962 \quad (4)$$

$$\text{At } 80\,^{\circ}\text{C}: W_{\text{flux}} = 0.0463F_{\text{air}} + 0.4932 \quad (5)$$

where F_{air} is air-flow rate (SLPM). Compared to the water flux without the GDL, the water flux with the hydrophobic GDL increases much more slowly with increasing flow rate. This can also be

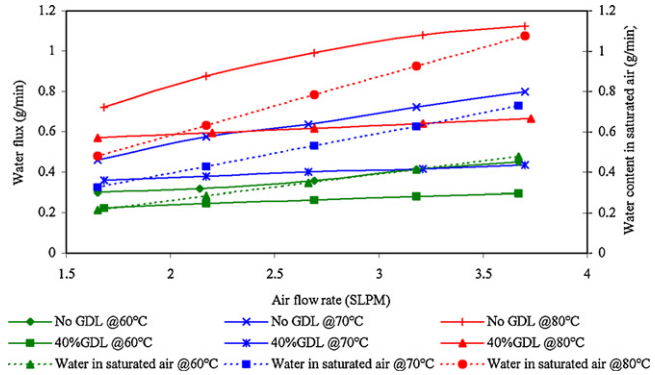

Fig. 3. Comparison of water flux using GDL treated by 40 wt% PTFE and without GDL under the condition of dry feed air; PEM: Nafion® 211CS, 7 cm × 7 cm; GDL: TORAY® TGPH-060, 40 wt% PTFE-treated GDL on the cathode and plain GDL on anode; anode: deionized water, cathode: dry air.

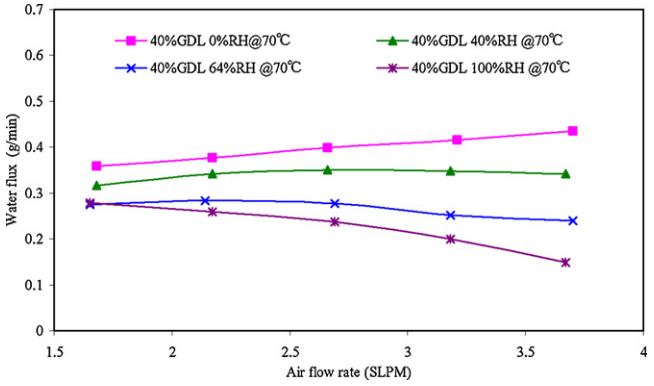

Fig. 4. Comparison of water flux under different air RHs at 70 °C; PEM: Nafion® 211CS, 7 cm × 7 cm; GDL: TORAY® TGPH-060, 40 wt% PTFE-treated GDL on the cathode and plain GDL on anode; anode: deionized water; cathode: air at different RHs.

explained by the high PTFE content in the GDL, which leads to a higher capillary pressure resulting in restrained water transport. Also, in Fig. 3, the intersections of the water fluxes and the curves of theoretical water content in saturated air at different temperatures provide the optimized flow rates for an operating PEM fuel cell when only the GDL is considered.

3.2. Effects of air temperature and humidity

To further discuss the effects of the GDL on water transport, measurements at different air humidification levels and temperatures were carried out with 40-wt% PTFE-treated GDL. When the feed air is humidified, the water collected in the experiment also includes the water contained in the humidified air prior to entering the cell. Therefore, the actual water flux is obtained by subtracting the amount of water originally contained in the humidified air from the water collected. Fig. 4 shows the water fluxes under different levels of air humidification at 70 °C.

At 70 °C and with humidified air, the water flux decreases with increasing flow rate, especially for the 100% RH (relative humidity) air feed, which demonstrates that less water is removed from the cell at even high flow rates. This indicates that increasing the flow rate does not always increase the performance of a PEM fuel cell. When the relative humidity of the feed air is high, the cell performance sometimes drops under high flow rates as more water is brought into the channels. Since the channels have limited water removal ability, the additional liquid water in the channels reduces the water removal efficiency, resulting in a decreased water flux at high flow rates.

3.3. Current density optimization

In this work, the measured water flux corresponds to the maximum capability of water removal at the cathode side, as the Nafion® 211CS membrane is fully hydrated by circulating water at the anode side. In an operating PEM fuel cell, if more water is generated at the cathode than the maximum water removal capability at certain flow rate, flooding occurs at the cathode side. And if the water removal capability at certain flow rate is much higher than the rate of water generation, the membrane is prone to drying and inferior performance.

Fig. 5 shows an example of the differentiation between the regions of possible drying and possible flooding under different air humidities at 70 °C and an air stoichiometry of 3.0. In Fig. 5, the dashed line is the theoretically calculated result for the rate of water generated by ORR as a function of current density at an air sto-

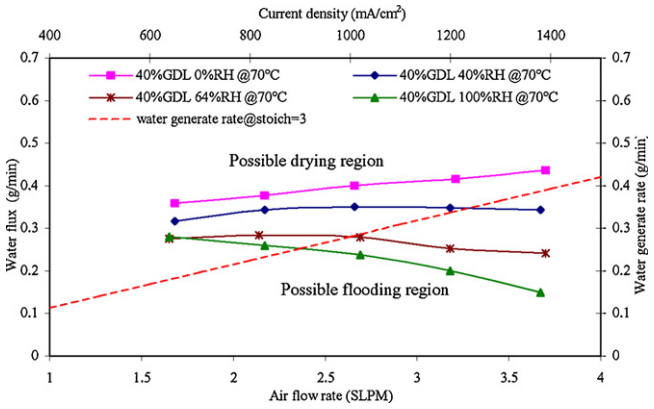

Fig. 5. Current density optimization at 70 °C and an air stoichiometric ratio = 3; PEM: Nafion® 211CS, 7 cm × 7 cm, GDL: TORAY® TGPH-060, 40 wt% PTFE-treated GDL on the cathode and plain GDL on anode; anode: deionized water; cathode: air at different RHs.

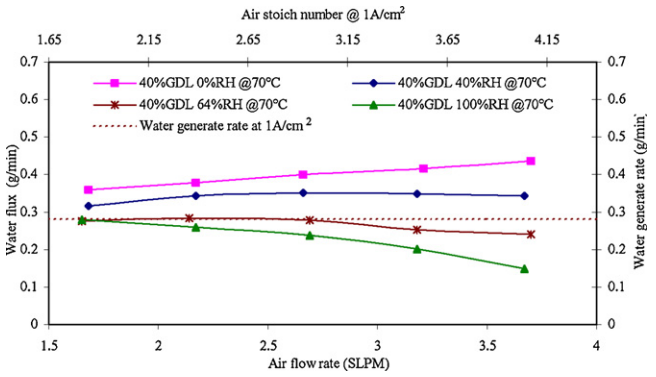

Fig. 6. Air-flow stoichiometry optimization at a current density of 1 A cm^{-2} at 70 °C; PEM: Nafion® 211CS, 7 cm × 7 cm, GDL: TORAY® TGPH-060, 40 wt% PTFE-treated GDL on the cathode and plain GDL on anode; anode: deionized water; cathode: air at different RHs.

ichiometry of 3.0. Above the dashed line, the measured water flux is higher than the water generated in the reaction, which means the generated water plus the water in the humidified air could be effectively removed and flooding would be avoided when operating a real PEM fuel cell. However, if the water flux is significantly higher than the rate of water generation, it will lead to membrane drying. For example, a PEM fuel cell operated at 600 mA^{-1} cm^{-2} using dry feed air with a stoichiometric number of 3.0 will probably cause dehydration of the membrane due to the doubled water removal capability compared to the water-generating rate at this current density. A higher current density may have the advantage of keeping water balance of water removal and generation under the condition of dry feed air. If a fuel cell is operated under conditions below the dashed line, the water removal capability of the air-flow cannot keep up with the water generating rate. Then, flooding is prone to happen. For instance, a PEM fuel cell operated at a current density higher than 1200 mA cm^{-2} using 100% RH feed air with a stoichiometric number of 3, will probably cause flooding of the cell for the given cell components. The preferred water-balanced operation region, where the water removal capability of the air-flow equals the water generated by ORR, can also be predicted in Fig. 5. For example, 1200 mA cm^{-2}, 1000 mA cm^{-2} and 900 mA cm^{-2} are the optimized current densities for the feed air RH of 40, 64 and 100%, respectively, based on Fig. 5. This method provides a useful tool to seek the possible flooding and drying operation regions, which should be avoided when operating a real PEM fuel cell, and to optimize the operating current densities under different humidification levels of the feed air.

3.4. Air stoichiometry optimization at a given current density

If the operational current density is given for a certain PEM fuel cell application, the rate of water generation is constant, and optimization of the air-flow could effectively avoid flooding, as well as drying. Stoichiometry ratio control is a widely used air-flow control method and Fig. 6 provides an example of optimizing the air-flow stoichiometry and feed air RH at a current density of 1 A cm^{-2} at 70 °C. As shown in Fig. 6, the dashed line is the theoretically calculated rate of water generation at 1 A cm^{-2} and the air-flow rate is converted to stoichiometry as shown in the secondary *X*-axis. It could be observed that when the stoichiometry is higher than 1.65, the water flux using dry and 40% RH air is higher than the rate of water generation at 1 A cm^{-2} and flooding is not prone to occur. However, if the air stoichiometry is higher than 3, the flowing air will remove too much water and result in membrane drying, especially with dry air. When 100% RH feed air is used, the water flux is lower than the water generation rate and flooding will occur at even high stoichiometries. 64% RH air seems to be the better choice when for a stoichiometry between 2 and 3 at 1 A cm^{-2}. The water flux and water generation rate are similar and the water in the fuel cell is easier to balance. This method is a useful tool to optimize the air stoichiometry number and feed air RH.

4. Conclusions

The water transported through the membrane and GDL was measured using a single PEM fuel cell with an active area of 50 cm^2. Various effects of the GDLs on water transport were investigated. It was found that the use of a hydrophobic GDL (40 wt% PTFE-treated) reduced the water flux at all temperatures. At or near fully saturated conditions, higher air-flow rates did not remove more water out of fuel cell as one may expect.

This paper provides some useful tools for determining the optimal operation conditions to avoid flooding and drying issues and it is applicable to different components within and designs of an operating PEM fuel cell. Further work is still needed to fully understand the effects of GDLs on mass transport. An investigation of the effects of different PTFE contents in GDLs and the effects of the micro-porous layer is ongoing and will be reported soon.

Acknowledgements

The authors acknowledge the NRC-Helmholtz Joint Research program, NRC-MOST Joint Research Program and BCIC's ICSD Program for financial support.

References

[1] T.A. Zawodzinski, C. Derouin, S. Radzinski, R.J. Sherman, V.T. Smith, T.E. Springer, S. Gottesfeld, J. Electrochem. Soc. 140 (1993) 1041–1047.
[2] B.S. Pivovar, Polymer 47 (2006) 4194–4202.
[3] G.Q. Lu, F.Q. Liu, C.Y. Wang, J. Power Sources 164 (2007) 134–140.
[4] F.Q. Liu, G.Q. Lu, C.Y. Wang, J. Membr. Sci. 287 (2007) 126–131.
[5] X.G. Yang, N. Burke, C.Y. Wang, K. Tajiri, K. Shinohara, J. Electrochem. Soc. 152 (2005) A759–A766.
[6] O. Himanen, T. Hottinen, M. Mikkola, V. Saarinen, Electrochim. Acta 52 (2006) 206–214.
[7] Q.G. Yan, H. Toghiani, J.X. Wu, J. Power Sources 158 (2006) 316–325.
[8] G.J.M. Janssen, M.L.J. Overvelde, J. Power Sources 101 (2001) 117–125.
[9] Y.H. Cai, J. Hu, H.P. Ma, B.L. Yi, H.M. Zhang, Electrochim. Acta 51 (2006) 6361–6366.
[10] K.-H. Choi, D.-H. Peck, C.S. Kim, D.-R. Shin, T.-H. Lee, J. Power Sources 86 (2000) 197–201.
[11] T. Murahashi, M. Naiki, E. Nishiyama, J. Power Sources 162 (2006) 1130–1136.
[12] X.H. Ye, C.Y. Wang, J. Electrochem. Soc. 154 (2007) B683–B686.

[13] M.V. Williams, H.R. Kunz, J.M. Fenton, J. Electrochem. Soc. 151 (2004) A1617–A1627.
[14] H. Nakajima, T. Konomi, T. Kitahara, J. Power Sources 171 (2007) 457–463.
[15] D. Bevers, R. Rogers, M. von Bradke, J. Power Sources 63 (1996) 193–201.
[16] L.R. Jordan, A.K. Shukla, T. Behrsing, N.R. Avery, B.C. Muddle, M. Forsyth, J. Power Sources 86 (2000) 250–254.
[17] G. Lin, T. Van Nguyen, J. Electrochem. Soc. 152 (2005) A1942–A1948.
[18] D.P. Wilkinson, M. Blanco, H. Zhao, J. Wu, H. Wang, Electrochem. Solid-State Lett. 10 (2007) B155–B160.
[19] T.A. Trabold, Heat Transfer Eng. 26 (2005) 3–12.
[20] J. Scholta, G. Escher, W. Zhang, L. Kuppers, L. Jorissen, W. Lehnert, J. Power Sources 155 (2006) 66–71.
[21] J.P. Owejan, T.A. Trabold, D.L. Jacobson, M. Arif, S.G. Kandlikar, Int. J. Hydrogen Energy 32 (2007) 4489–4502.
[22] X.G. Li, I. Sabir, J. Park, J. Power Sources 163 (2007) 933–942.
[23] M.V. Williams, E. Begg, L. Bonville, H.R. Kunz, J.M. Fenton, J. Electrochem. Soc. 151 (2004) A1173–A1180.
[24] C.S. Kong, D.-Y. Kim, H.-K. Lee, Y.-G. Shul, T.-H. Lee, J. Power Sources 108 (2002) 185–191.
[25] L.R. Jordan, A.K. Shukla, T. Behrsing, N.R. Avery, B.C. Muddle, M. Forsyth, J. Appl. Electrochem. 30 (2000) 641–646.
[26] J.I. Gostick, M.A. Ioannidis, M.W. Fowler, M.D. Pritzker, J. Power Sources 173 (2007) 277–290.
[27] J.T. Gostick, M.W. Fowler, M.D. Pritzker, M.A. Ioannidis, L.M. Behra, J. Power Sources 162 (2006) 228–238.
[28] U. Pasaogullari, C.-Y. Wang, K.S. Chen, J. Electrochem. Soc. 152 (2005) A1574–A1582.
[29] P. Ugur, C.Y. Wang, J. Electrochem. Soc. 151 (2004) A399–A406.
[30] U. Pasaogullari, C.-Y. Wang, Electrochim. Acta 49 (2004) 4359–4369.
[31] S. Maharudrayya, S. Jayanti, A.P. Deshpande, J. Fuel Cell Sci. Technol. 4 (2007) 357–364.
[32] G.-G. Park, Y.-J. Sohn, T.-H. Yang, Y.-G. Yoon, W.-Y. Lee, C.-S. Kim, J. Power Sources 131 (2004) 182–187.
[33] K. Karan, H. Atiyeh, A. Phoenix, E. Halliop, J. Pharoah, B. Peppley, Electrochem. Solid-State Lett. 10 (2007) B34–B38.
[34] H.K. Atiyeh, K. Karan, B. Peppley, A. Phoenix, E. Halliop, J. Pharoah, J. Power Sources 170 (2007) 111–121.
[35] X.L. Wang, H.M. Zhang, J.L. Zhang, H.F. Xu, Z.Q. Tian, J. Chen, H.X. Zhong, Y.M. Liang, B.L. Yi, Electrochim. Acta 51 (2006) 4909–4915.
[36] J.H. Nam, M. Kaviany, J. Int. Heat Mass Transfer 46 (2003) 4595–4611.
[37] M. Mathias, J. Roth, J. Fleming, W. Lehnert, W. Vielstich, A. Lamm, HG (Eds.), Handbook of Fuel Cells, vol. 3, Wiley & Sons Ltd, Chichester, England, 2003, pp. 1–21.
[38] E. Passalacqua, G. Squadrito, F. Lufrano, A. Patti, L. Giorgi, J. Appl. Electrochem. 31 (2001) 449–454.
[39] J. Chen, T. Matsuura, M. Hori, J. Power Sources 131 (2004) 155–161.
[40] E. Antolini, A. Pozio, L. Giorgi, E. Passalacqua, J. Mater. Sci. 33 (1998) 1837–1843.
[41] Z. Qi, A. Kaufman, J. Power Sources 109 (2002) 38–46.
[42] E. Antolini, R.R. Passos, E.A. Ticianelli, J. Appl. Electrochem. 32 (2002) 383–388.
[43] X. Zhu, P.C. Sui, N. Djilali, J. Power Sources 172 (2007) 287–295.
[44] D. Spernjak, A.K. Prasad, S.G. Advani, J. Power Sources 170 (2007) 334–344.
[45] T. Ous, C. Arcoumanis, J. Power Sources 173 (2007) 137–148.
[46] A. Bazylak, D. Sinton, Z.S. Liu, N. Djilali, J. Power Sources 163 (2007) 784–792.
[47] F.Y. Zhang, X.G. Yang, C.Y. Wang, J. Electrochem. Soc. 153 (2006) A225–A232.
[48] Z.G. Zhan, J.S. Xiao, M. Pan, R.Z. Yuan, J. Power Sources 160 (2006) 1–9.